Effect of Nonisothermal Operation on Catalyst Fouling

MITSUO SAGARA, SHINOBU MASAMUNE, and J. M. SMITH

University of California, Davis, California

The time rate of change of catalyst effectiveness factors was considered by Masamune and Smith (*1*) at isothermal conditions. While the rate of energy evolution due to the fouling reaction will probably always be unimportant, the heat of the main reaction may cause significant intraparticle temperature gradients. These intrapellet temperature profiles will influence the rate of fouling and, as shown later, may cause striking changes in the effectiveness factor.

It is supposed that the only effect of fouling is to reduce the active surface of the catalyst, for example, by deposition of an inert material. Also both the main reaction

$$A \rightarrow B \tag{1}$$

and the fouling reactions are taken as first order. For parallel fouling the deposited substance, C, is formed by

$$A \rightarrow C(s) \tag{2}$$

and for series fouling by the reactions

$$A \rightarrow B \rightarrow C(s) \tag{3}$$

Under these conditions the rate of deposition of $C(s)$ is

$$\frac{\partial q}{\partial t} = k_{A,f}\,(1-\psi)\,C_A \tag{4}$$

for parallel fouling, and

$$\frac{\partial q}{\partial t} = k_{B,f}\,(1-\psi)\,C_B \tag{5}$$

for series fouling. Here $\psi = q/q_o$, the fraction of the surface that is fouled (inactive).

Equations (4) or (5) can be combined with differential mass and energy balances to determine the concentration of reactant A as a function of time and position in the catalyst pellet. In the isothermal work (*1*) time-dependent effectiveness factors for spherical catalyst pellets were presented as a function of intrapellet diffusion resistance. The same procedure will be used here for the nonisothermal case. The results are influenced by additional parameters β, γ, and γ_f which involve the heat of the main reaction and the activation energies of the main and fouling reactions. The details of the mathematical development need not be presented. It is sufficient to give the differential mass and energy balances and point out the unique features of the method of solution.

Since the fouling reaction is assumed to proceed much more slowly than the main reaction, a pseudo-steady state can be assumed for the latter. Then the mass and energy balances may be written

$$\frac{1}{r^2}\frac{\partial}{\partial r}\left(r^2\,D_A\frac{\partial C_A}{\partial r}\right) - \rho\,k_A\,(1-\psi)\,C_A = 0 \tag{6}$$

$$\frac{1}{r^2}\frac{\partial}{\partial r}\left(r^2\,D_B\frac{\partial C_B}{\partial r}\right) + \rho\,k_A\,(1-\psi)\,C_A = 0 \tag{7}$$

$$\frac{1}{r^2}\frac{\partial}{\partial r}\left(r^2\,k_e\frac{\partial T}{\partial r}\right) + (-\Delta H)\,\rho\,k_A\,(1-\psi)\,C_A = 0 \tag{8}$$

The rate of reaction expression in Equations (6) and (7) is similar to Equation (4) except the rate constant k_A applies to the main reaction.

Equations (6) to (8) and (4) or (5), with appropriate boundary conditions establish the profiles of C_A, C_B, T, and ψ within the catalyst pellet as a function of time. Equations (6) and (7) can be combined to eliminate the reaction term and then integrated to obtain a linear relationship between C_A and C_B. Similarly Equations (6) and (8) lead to the linear Damkoehler relationship between C_A and T. These results can be used to express k_A, which is equal to $A_A\,e^{-E/RT}$, in terms of C_A. Then Equation (6) contains only C_A and ψ as dependent variables. A similar procedure can be used to express $k_{A,f}$ or $k_{B,f}$ in Equations (4) and (5) in terms of C_A or C_B instead of T. The result is that the complex system of equations can be reduced, for each type of fouling, to two differential equations describing C_A and ψ as a function of time and radial position in the pellet. The first equation, arising from Equation (6), can be written in dimensionless form as

$$\frac{\partial^2\Phi_A}{\partial\xi^2} + \frac{2}{\xi}\frac{\partial\Phi_A}{\partial\xi} - h^2\Phi_A\,(1-\psi)\exp\left[\frac{\gamma\beta(1-\Phi_A)}{1+\beta(1-\Phi_A)}\right] = 0 \tag{9}$$

The second equation depends upon the type of fouling, and for the parallel case it is

$$\frac{\partial\psi}{\partial\theta_A} = \Phi_A\,(1-\psi)\exp\left[\frac{\gamma_f\beta(1-\Phi_A)}{1+\beta(1-\Phi_A)}\right] \tag{10}$$

and for series fouling

$$\frac{\partial\psi}{\partial\theta_B} = [1+\epsilon\,(1-\Phi_A)]\,(1-\psi)\exp\left[\frac{\gamma_f\,\beta(1-\Phi_A)}{1+\beta(1-\Phi_A)}\right] \tag{11}$$

The dimensionless parameters and variables are defined as follows:

$$\Phi_A = C_A/C_{Ao} \tag{12}$$

$$\Phi_B = C_B/C_{Bo} \tag{13}$$

$$\psi = \frac{q}{q_o} \tag{14}$$

$$\xi = r/r_o \tag{14a}$$

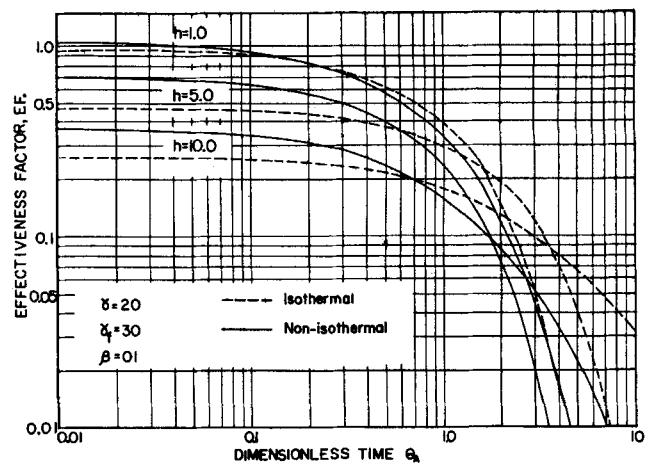

Fig. 1. Effectiveness factors for parallel fouling.

Shinobu Masamune is with Mitsubishi Petrochemical Company, Tokyo, Japan.

$$\theta_A = \frac{t k_{A,fo} C_{A_o}}{q_o}; \quad [k_{A,fo} = A_{A,f} \exp(-E_f/RT_o)] \quad (15)$$

$$h = r_o \sqrt{\frac{\rho k_{A_o}}{D_A}}; \quad [k_{A_o} = A_A \exp(-E_A/RT_o)] \quad (16)$$

$$\gamma = \frac{E}{RT_o}; \quad \gamma_f = \frac{E_f}{RT_o} \quad (17)$$

$$\beta = \frac{(-\Delta H)\, D_A\, C_{A_o}}{k_e\, T_o} \quad (18)$$

For series fouling the following definitions are also needed:

$$\theta_B = \frac{t\, k_{B,fo}\, C_{B_o}}{q_o}; \quad [k_{B,fo} = A_{B,f} \exp(-E_f/RT_o)] \quad (19)$$

$$\epsilon = \frac{D_A\, C_{A_o}}{D_B\, C_{B_o}} \quad (20)$$

The boundary conditions are

$$\psi = 0 \text{ at } \theta = 0 \text{ for } 1 \geq \xi \geq 0 \quad (21)$$

$$\Phi_A = 1 \text{ at } \xi = 1 \text{ for } \theta \geq 0 \quad (22)$$

$$\frac{\partial \Phi_A}{\partial \xi} = 0 \text{ at } \xi = 0 \text{ for } \theta \geq 0 \quad (23)$$

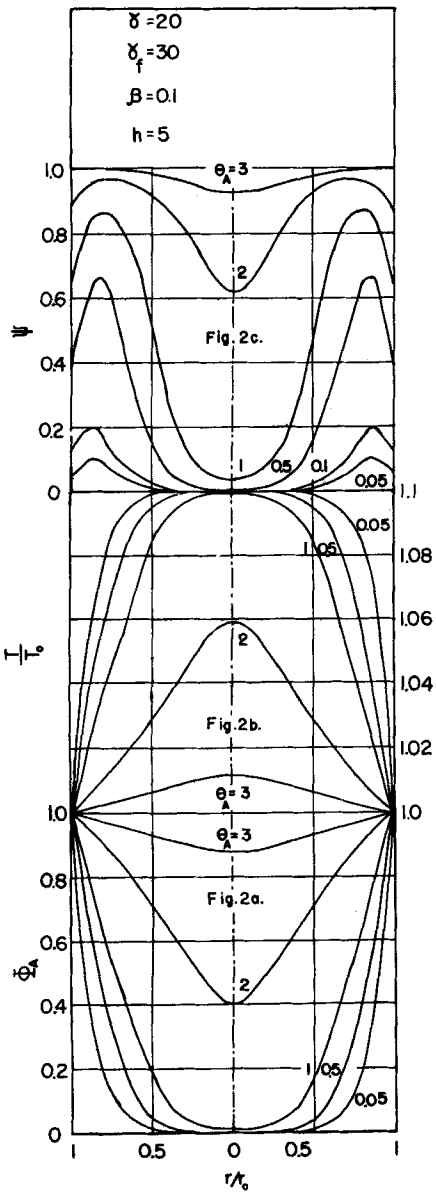

Fig. 2. Radial profiles for parallel fouling.

SOLUTION METHOD

The numerical solution of Equations (9) and (10) or (9) and (11) is complicated because the exponential term makes convergence difficult, particularly at high activation energies. We found the quasilinearization technique of Lee (2) to be helpful. In this method the reaction, or exponential, term in Equation (9) is expanded in a Taylor series with respect to Φ_A. If the series is terminated after the second term, and R is used to represent the reaction term in Equation (9)

$$R[\Phi_A(k+1)] = R[\Phi_A(k)] + R'[\Phi_A(k)]\,[\Phi_A(k+1) - \Phi_A(k)] \quad (24)$$

where k is an iteration number. With this procedure the values of Φ_A, at any time and position increment, converged after two or at most three iterations. The method was to substitute R from Equation (24) into Equation (9), thus eliminating the exponential term. Then conventional difference methods were used to obtain a numerical solution (IBM 7044 computer) for Φ_A as a function of time and radial position within the pellet. Once Φ_A was established, C_B and the temperature were readily evaluated from the linear relationships previously obtained by solution of pairs of Equations (6) to (8).

The effect of fouling can be concisely shown by calculating a catalyst effectiveness factor $E.F.$ based upon the initial conditions at the outer surface of the pellet. This was calculated from the defining equation

$$E.F. \equiv \frac{4\pi r_o^2\, D_A \left(\frac{\partial C_A}{\partial r}\right)_{r=r_o}}{\frac{4}{3}\pi r_o^3\, \rho\, k\, C_{A_o}} = \frac{3}{h^2}\left(\frac{\partial \Phi}{\partial \xi}\right)_{\xi=1} \quad (25)$$

$E.F.$ depends upon time because the concentration gradient at the outer surface varies with t.

RESULTS

Parallel Fouling

The solid lines in Figure 1 illustrate how the effectiveness factor decreases with increasing time θ_A for parallel fouling. Typical values of parameters for an exothermic main reaction $\beta = +0.10$ were chosen. The Arrhenius number γ is 20 for the main reaction and 30 for the fouling reaction, corresponding to activation energies of about

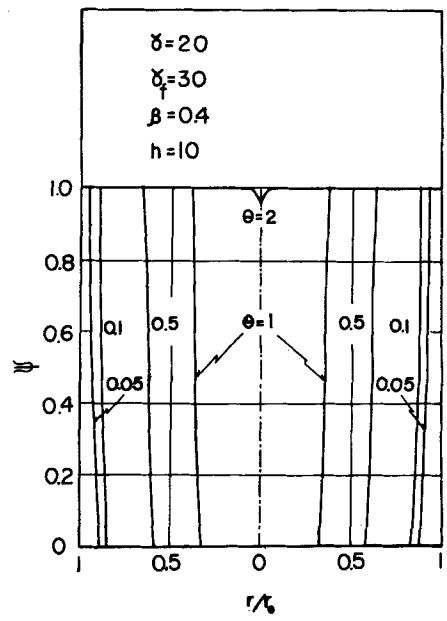

Fig. 3. Radial profile of ψ for high β and h. (parallel fouling).

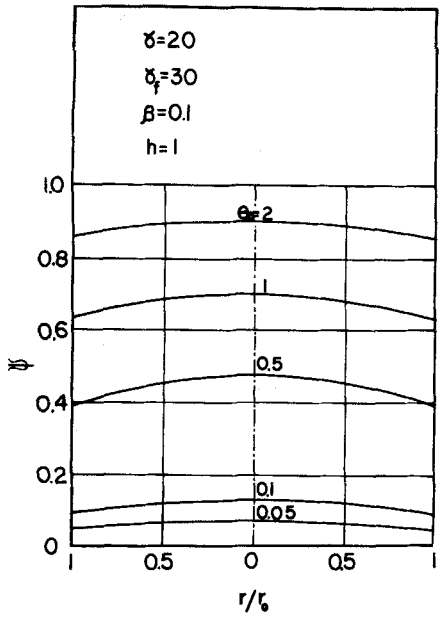

Fig. 4. Radial profile of ψ for low diffusion resistance and low β (parallel fouling).

20 kcal/g.-mole and 30 kcal/g.-mole, respectively, at a surface temperature of 500°K. The dotted lines represent the results for the isothermal case (*1*) for the same h values. Comparison of *E.F.* values from the solid and dotted lines at the same θ_A gives the effect of nonisothermal conditions. The nonisothermal curves at low θ_A are higher because the exothermic reaction causes the temperature (and rate of reaction) to increase toward the center of the relatively clean pellet. At higher θ_A, fouling becomes significant, and its effect on the rate more than offsets the favorable effect of the temperature rise. Hence the isothermal and nonisothermal curves ultimately cross. Since diffusion resistance reduces the concentration of A within the pellet, fouling will also be reduced as h increases. This means that the curves cross at longer times for larger values of the Thiele modulus. At $\theta_A = 0$ there is no fouling, $\psi = 0$. The solid lines at $\theta_A = 0.01$ in Figure 1 approach this condition. The effectiveness factors here agree with those presented by Weisz and Hicks (*3*) for nonisothermal, clean catalyst behavior.

The interaction of temperature and diffusion resistance on the extent of fouling leads to complex radial profiles of ψ. Figures 2 *a*, *b*, and *c* show the profiles of temperature, concentration, Φ_A, and ψ for the conditions of Figure 1 and an intermediate diffusion resistance corresponding to $h = 5$. The sharp drop in concentration of reactant, from the surface in toward the center of the pellet at low θ_A, reflects the intrapellet diffusion resistance. The somewhat analogous increase in temperature within the pellet is shown in Figure 2*b*. The counteracting effects of these two properties on the rate of the fouling reaction lead to the unusual profiles of ψ in Figure 2*c*. Proceeding inward from the outer surface, the effect of the increase in temperature more than offsets that of the decrease in concentration so that the rate of fouling and ψ both increase. Further into the pellet the concentration effect is dominant. Hence ψ goes through a maximum and then decreases toward the center of the pellet. As time increases the maximum is less sharp and ultimately disappears, for example at $\theta_A = 3$ in Figure 2*c*. The shell model, which assumes a completely fouled outer layer moving inwards with time, obviously would not be satisfactory for the conditions describing Figures 2*a*, *b*, and *c*.

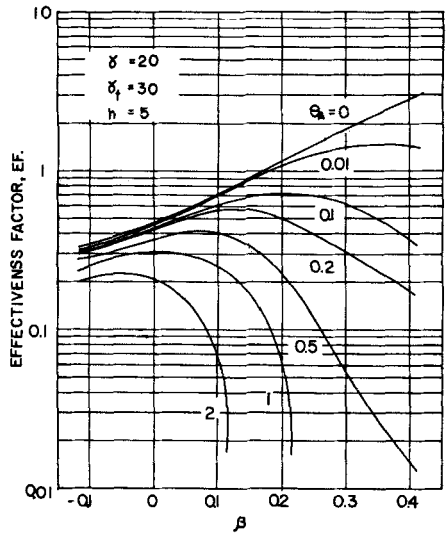

Fig. 5. Effect of heat of reaction for parallel fouling.

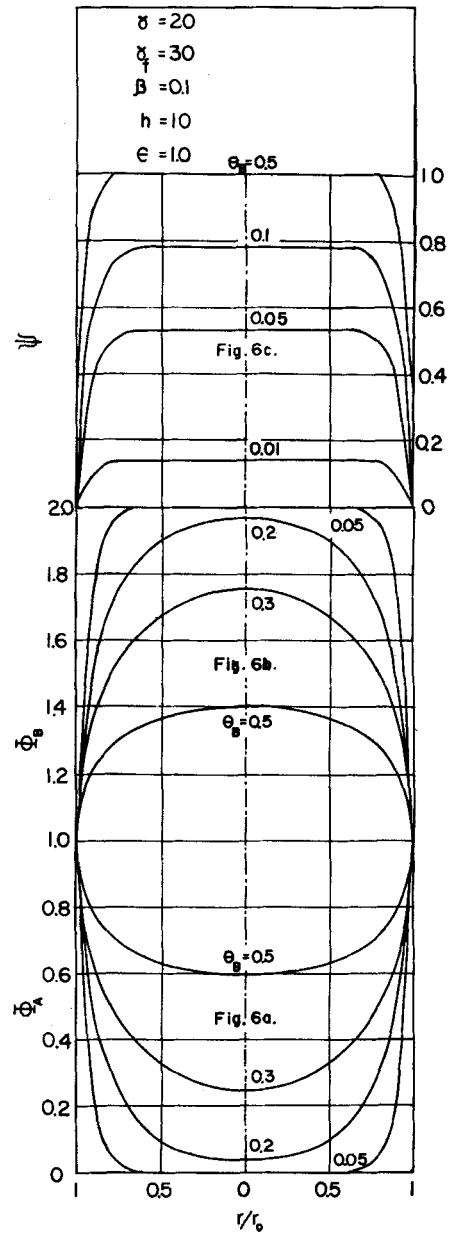

Fig. 6. Radial profiles for series fouling.

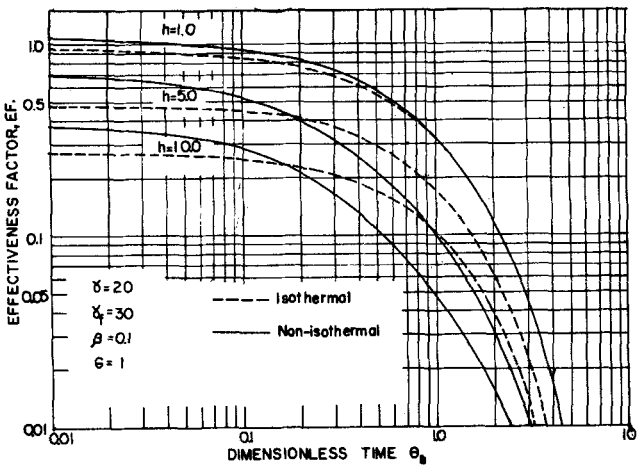

Fig. 7. Effectiveness factors for series fouling.

For a more highly exothermic main reaction (higher β) and for greater diffusion resistance (larger h) the shell model is a reasonable approximation for the nonisothermal case. This is illustrated in Figure 3 for the same conditions as Figure 2 except $\beta = 0.4$ and $h = 10$. Now the temperature rise is so large and the drop in reactant concentration so steep, in moving in from the pellet surface, that fouling is complete at a relatively sharp boundary. Therefore the plot of ψ consists of a nearly vertical line, moving with time toward the center of the pellet.

The importance of diffusion resistance on the profile of ψ is evident by comparing Figures 2*c* and 4. Figure 4 is based upon the same values of the parameters as Figure 2 except h is reduced to 1.0. With this low diffusion resistance, the extent of fouling is nearly uniform across the entire radius of the pellet.

The heat of reaction has a strong influence on *E.F.* as shown in Figure 5 for an intermediate diffusion resistance, $h = 5$. The curve for $\theta = 0$ is the same as that of Weisz and Hicks (3). For a highly exothermic reaction this figure illustrates that fouling can cause an order of magnitude decrease in effectiveness factor in a reasonable range of θ_A.

Series Fouling

In this case fouling is due to product B [see Equation (3)] and its concentration will be greatest at the center of the pellet. Therefore the effects of temperature and concentration of reactant, which opposed each other in parallel fouling, now are complementary. Both factors cause increased fouling towards the center. The resulting ψ profile is illustrated in Figure 6*c* for the indicated values of the parameters. In series fouling the ratio defined by ϵ plays a role and in Figure 6, $\epsilon = 1.0$. Figures 6*a* and *b* show the corresponding concentration profiles Φ_A and Φ_B. Effectiveness factors are compared with isothermal results for the same values of the parameters in Figure 7. As for parallel fouling, the nonisothermal and isothermal curves cross at higher values of θ_B. However, for the series case, a large diffusion resistance increases the concentration of B within the pellet and thereby increases the extent of fouling. Therefore an increase in Thiele modules causes the curves to cross at shorter times.

The procedures as outlined can be used to predict the effect of catalyst fouling (due to surface deactivation) for any values of intrapellet diffusivity, reaction rate constants, and heat of reaction. The method was illustrated for first order main and fouling reactions. An interesting result is that the "shell model" does not represent the exothermic reaction case very well unless the heat of reaction and Thiele modules are both relatively large. Illustrative calculations also show that effectiveness factors evaluated under isothermal conditions can be either greater or less than those which reflect the actual temperature profiles, depending upon the time of reaction. Finally, the quasilinearization technique of Lee (2) was found to be an accurate and efficient way of obtaining a convergent, numerical solution for an exponential form of nonlinearity.

ACKNOWLEDGMENT

The authors wish to acknowledge the financial assistance of the American Chemical Society (Petroleum Research Fund Project No. 1633).

NOTATION

A = gaseous reactant
B = gaseous product of main reaction
$C(s)$ = fouling substance deposited on the catalyst surface
C_A = concentration of A in pores of catalyst, g.-mole/cc.
C_{Ao} = concentration at r_o
D_A = effective diffusivity of A within the spherical catalyst particle, sq.cm./sec. (based upon void plus non-void area)
$E.F.$ = effectiveness factor for the pellet
h = Thiele modulus, defined by Equation (16)
ΔH = heat of reaction, cal./g.-mole
k_A = rate constant of main reaction, cc./(sec.)(g.-catalyst)
k_{Ao} = rate constant at T_o
$k_{A,f}$ = parallel fouling rate constant; cc./(sec.)(g.-catalyst)
$k_{A,fo}$ = rate constant at T_o
$k_{B,f}$ = series fouling rate constant, cc./(sec.)(g.-catalyst)
q = concentration of $C(s)$ on catalyst
q_o = maximum concentration corresponding to complete deactivation; g.-moles/(g.-catalyst)
R = dimensionless rate of main reaction,

$$\Phi_A\,(1-\psi)\,\exp\frac{\gamma\beta(1-\Phi_A)}{1+\beta(1-\Phi_A)}$$

r = radial distance from center
r_o = radius of pellet, cm.
t = process time, sec.
T = temperature in particle, T_o — temperature at r_o, °K.

Greek Symbols

β = parameter defined by Equation (18)
γ = Arrhenius number for main reaction, Equation (17)
γ_f = Arrhenius number for fouling reaction, Equation (17)
ϵ = dimensionless parameter defined by Equation (20)
θ = dimensionless time; θ_A, θ_B are defined by Equations (15) and (19)
k_e = effective thermal conductivity of catalyst particle, cal./(cm.)(sec.)(°C.)
ρ = density of catalyst pellet, g./cc.
ξ = r/r_o
Φ_A = C_A/C_{Ao}
Φ_B = C_B/C_{Bo}
ψ = q/q_o

Subscripts

$A, B,$ = gaseous components of reaction
f = fouling reaction
k = iteration number in quasi linearization
o = outer surface of catalyst particle

LITERATURE CITED

1. Masamune, Shinobu, and J. M. Smith, *AIChE J.*, **12**, 384 (1966).
2. Lee, E. S., *Chem. Eng. Sci.*, **21**, 183 (1966).
3. Weisz, P. B., and J. S. Hicks, *ibid.*, **17**, 265 (1962).